We have given no illustration of the use of the more complicated addition theorem (24) for $|f(\mathbf{q})f(\mathbf{q}')|$. We plan to use this result in an impact parameter calculation to examine the validity of Born approximation for the charge-exchange cross section $\sigma(\langle n_1 \rangle | n_2)$ for various values of n_1 and n_2.

Measurements of Electron Capture in Close H+-on-He and He+-on-H Collisions*

HERBERT F. HELBIG AND EDGAR EVERHART

Physics Department, University of Connecticut, Storrs, Connecticut

(Received 4 June 1964)

Differential measurements of electron capture probability P_0 are made for close encounters in the reaction $H^+ + He \rightarrow H + He^+$. The energy range of the incident proton is 1.6 to 180.0 keV and the scattering angle is varied from $\frac{1}{2}$ to $4°$. The impact parameters associated with these collisions extend from 0.015 to about 0.50 Å. There is little angular dependence to the data. When P_0 is plotted versus energy, a damped resonant structure is seen with peaks at 36, 7, and 2.6 keV with amplitudes of 0.52, 0.16, and 0.05, respectively. The phenomena are discussed in terms of the energy-level diagram for HeH+ and with reference to the existing theories for charge transfer in the nonresonant case. Measurements of the inverse reaction, He+ ions incident on atomic hydrogen targets, are also presented and discussed.

1. INTRODUCTION

R ESONANT electron capture in violent (or close) single encounters in symmetrical or "resonant" ion-atom systems has been studied in several experiments[1] and the pertinent theory[2-4] explains many of the observed features. However, a somewhat similar phenomenon found in the unsymmetrical or "nonresonant" reaction

$$H^+ + He \rightarrow H + He^+, \quad (\Delta E = +11 \text{ eV}), \quad (1)$$
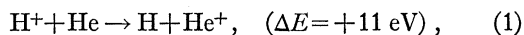
is not well understood.

Differential scattering measurements of the above reaction were first made by Ziemba et al.[5] These covered the energy range of 2 to 180 keV. The incident protons were driven through the electronic structure of helium atoms at impact parameters sufficiently small to deflect

the fast particles through an angle of 5°. The probability P_0 of electron capture by a proton in such a single collision was measured. When P_0 was plotted versus incident energy T, a damped resonant structure was seen.

The purpose of the present study is to repeat these measurements of H+ on He collision with considerably improved accuracy, and further, to study the angular dependence as well as the energy dependence of the quantity P_0, thus varying both the impact parameter and the velocity of the collision.

In addition, similar measurements of the inverse reaction,

$$He^+ + H \rightarrow He + H^+, \quad (\Delta E = -11 \text{ eV}), \quad (2)$$
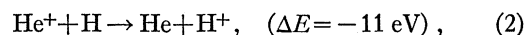
are also studied here, making use of the atomic hydrogen target chamber previously developed for the H+ on H studies.[1]

There is, at present, no published theory in a form readily applicable to the reactions (1) and (2) under study here. The general theory of charge transfer in nonresonant collisions is that of Bates, Massey, and Stewart[6] as improved by Takayanagi,[7] and Bates and McCarroll.[8] Further contributions by Bates and Lynn,[9]

---

* This work was supported by the U. S. Army Research Office, Durham.

[1] Experiments on symmetrical case: H+ on H: G. J. Lockwood and E. Everhart, Phys. Rev. **125**, 567 (1962). He+ on He: Data from 0.4 to 250 keV, G. J. Lockwood, H. F. Helbig, and E. Everhart, Phys. Rev. **132**, 2078 (1963); data from 0.03 to 0.60 keV, W. Aberth and D. C. Lorents (to be published), and Bull. Am. Phys. Soc. **9**, 427 (1964). Ne+ on Ne: P. R. Jones, P. Costigan, and G. Van Dyk, Phys. Rev. **129**, 211 (1963). Ar+ on Ar: P. R. Jones, in *Proceedings of the Third International Conference of the Physics of Electronic and Atomic Collisions*, edited by M. R. C. McDowell (North-Holland Publishing Company, Amsterdam, 1964). H₂+ on H₂, Ne+ on Ne, Kr+ on Kr: See Ref. 5 below.

[2] D. R. Bates and R. McCarroll, Advan. Phys. **11**, 39 (1962); See also Refs. 6 and 8.

[3] W. L. Lichten, Phys. Rev. **131**, 229 (1963).

[4] E. Everhart, Phys. Rev. **132**, 2083 (1963). References 2–4 list many other papers concerned with the symmetrical case.

[5] F. P. Ziemba, G. J. Lockwood, G. H. Morgan, and E. Everhart, Phys. Rev. **118**, 1552 (1960), See Fig. 4(c) and Sec. 4c for early H+ on He data.

[6] D. R. Bates, H. S. W. Massey, and A. L. Stewart, Proc. Roy. Soc. (London) **A216**, 437 (1953). See, particularly, Eqs. (120) to (129) on p. 454.

[7] K. Takayanagi, Sci. Repts. Saitama Univ. (Japan) **2A**, 33 (1955).

[8] D. R. Bates and R. McCarroll, Proc. Roy. Soc. (London) **A245**, 175 (1958). See particularly Eqs. (12) to (18) p. 177.

[9] D. R. Bates and N. Lynn, Proc. Roy. Soc. (London) **A253**, 141 (1959).

by Rapp and Francis,[10] by Demkov,[11] and by Lichten,[12] all treat the nonresonant case and present partially relevant or approximate solutions.

Section 2 below describes the experiment and presents the data. Section 3 discusses the wave functions and energies of HeH^+ and Li^+ which enter into an adiabatic description of reactions (1) and (2) under study here. Section 4 discusses the data, relating it to the several theories. Finally, in Sec. 5 the present differential cross-section measurements are discussed in relation to total cross-section data.

2. EXPERIMENT AND DATA

In these experiments, an incident beam of ions (H^+) is passed through a low-density target gas (He). Collimating holes are arranged so that those incident particles which are scattered to an angle θ (in a single collision) may be counted according to their charge state (H^+ or H°) after scattering. The fraction of these scattered particles which are neutral is P_0, which is the probability of electron capture in a single collision. The apparatus for the present H^+ on He study is identical to that described in the previous study of He^+ on He collisions by Lockwood et al.[1]

Measurements of P_0 in H^+ on He collisions were made between energies of 1.6 and 180.0 keV, and at scattering angles between $\frac{1}{2}$ and $4°$. Figure 1 shows the energy dependence of P_0 for data taken at various fixed scattering angles. There is surprisingly little angular variation with respect to the location of the peaks and valleys or their amplitudes. These data are discussed in Sec. 4b below.

A second experiment studied He^+ on H collisions with the same apparatus. Production of the atomic hydrogen target gas required use of a tungsten furnace as a target gas chamber, as described by Lockwood and Everhart.[1]
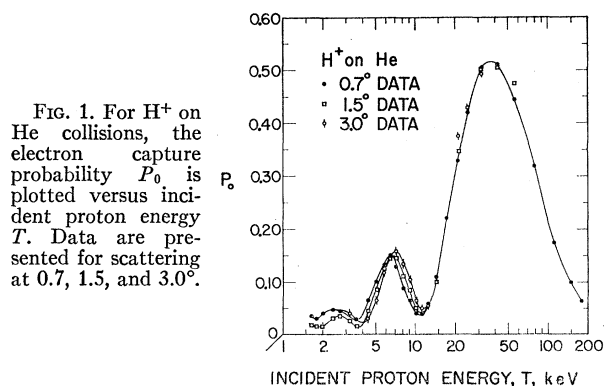

FIG. 1. For H^+ on He collisions, the electron capture probability P_0 is plotted versus incident proton energy T. Data are presented for scattering at 0.7, 1.5, and 3.0°.
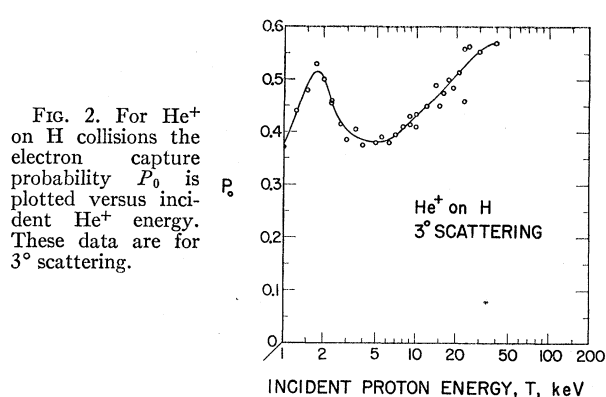

FIG. 2. For He^+ on H collisions the electron capture probability P_0 is plotted versus incident He^+ energy. These data are for 3° scattering.

A further paper by Lockwood, Helbig, and Everhart[13] discusses quantitative measurements of the dissociation fraction of hydrogen in such a furnace.

Figure 2 shows the energy dependence of P_0 for He^+ on H collisons, wherein the incident helium is scattered through a fixed angle of 3°. In this case data were not taken at other scattering angles. This reaction is discussed in Sec. 4c below.

3. ENERGY LEVELS OF HeH$^+$

Before it is possible to relate the data to the theories, it is necessary to look at the correlations and energy level diagram for HeH^+ at all internuclear separations. The several theories[6–12] require a detailed knowledge of these energy levels and the corresponding wave functions. These energy levels will be used in part b below to obtain an approximate relationship between scattering angle θ and distance of closest approach R_0, and in Sec. 4, they will be used in discussing the transitions which may occur during the collision.

(a) HeH$^+$ Energies

The energy levels of the HeH^+ system are shown in Fig. 3, plotted versus internuclear separation R. This diagram does not include the Coulomb term, and at $R=0$, the energies are those of Li^+. The ground state marked "A" is a singlet state. At $R=\infty$, it describes $H^+ + He$ $(1s)^2$. At intermediate values of R, it is the lowest $^1\sum$ state of HeH^+, and at $R=0$, it is the Li^+ $(1s)^2$ state. There are two excited states which reduce to H $(1s) + He^+$ $(1s)$ at $R=\infty$. The singlet state marked "B" reduces to singlet Li^+ $(1s2s)$ at $R=0$, and the triplet state marked "C" reduces to triplet Li^+ $(1s2s)$ at $R=0$. The next higher singlet and triplet states are marked "D" and "E," respectively. These are uncertain where shown dashed. Higher states and their correlations are not shown.

The energy levels of the ground state have been com-

[10] D. Rapp and W. E. Francis, J. Chem. Phys. 37, 2631 (1962). See Secs. IV and V. See also E. F. Gurnee and J. L. Magee, J. Chem. Phys. 26, 1237 (1957).

[11] Yu. N. Demkov, Zh. Eksperim. i Teor. Fiz. 45, 195 (1963) [English transl.: Soviet Phys.—JETP 18, 138 (1964)].

[12] W. L. Lichten (private communication); see also Ref. 3, Eqs. (1)–(11).

[13] G. J. Lockwood, H. F. Helbig, and E. Everhart, J. Chem. Phys. (to be published).
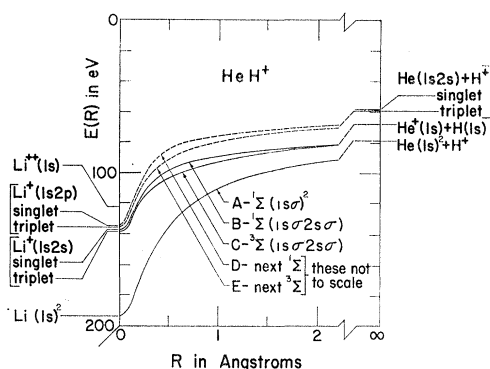
FIG. 3. The electronic energies E of several states of the HeH$^+$ system are plotted versus interatomic separation R. These values are taken entirely from the work of H. H. Michels, Ref. 18.

puted by Evett,[14] Bhattacharya[15] (including first excited state), Anex,[16] and Michels and Harris.[17] These calculations[14–17] have been concerned with the larger values of R. Energies of the ground state at small values of R and detailed calculations of the many excited states at all values of R have been computed by Michels,[18] who makes a variational calculation with a superposition of flexible one-electron wave functions in an elliptic coordinate system. Figure 3 is taken entirely from Michels' results and his work should be referred to for accurate numerical values.

There is always one electron close to the helium nucleus, so that the wave function of the other electron is something like that of a single electron in the neighborhood of the two centers He$^+$ and H$^+$. This is evident from Michels' wave functions, and the functions are also pictured in Miss Battacharya's paper.[15] There is also a qualitative resemblance to the corresponding wave functions of HeH^{2+} as drawn by Bates and Carson.[19]

The correlations between the states in Fig. 3 and higher states not shown here have also been worked out by Lichten[12] and by Green.[20]

(b) Relationship between θT and R_0

The interatomic energy is approximately

$$V(R) = 2/R + E(R) - E(\infty), \qquad (3)$$

where $E(R)$ is the (negative) electronic energy at R and $E(\infty)$ is the (negative) energy at infinity. If the collision were elastic and adiabatic, then (singlet) state "A" of

Fig. 3 could be used for $E(R)$. However, if a transition occurs to the (singlet) state "B" at some point, the value of $E(R)$ changes accordingly. In the present case, where there are periodic transitions between the states "A" and "B" during the collision, the average electronic energy must lie somewhere in between. In fact, there is not an exact one-to-one correspondence between the scattering angle and impact parameter because the potential energy for any given encounter depends upon the combination of transitions between states "A" and "B" which occurs before the scattered particle emerges. There is also a question as to whether it is appropriate to use elastic scattering formulas to calculate scattering angles in cases where there is inelastic energy loss.

For small-angle scattering, the relationship between θ and R_0 is readily obtained from $V(R)$. The formulas and calculation procedure are described in Sec. 3 (b,c) of Ref. 4, which also points out that R_0 is a function only of the product θT (where T is the incident energy). Taking for $E(R) - E(\infty)$ the energies of state "A" of Fig. 3, the calculation is carried out and then is repeated for state "B." The results are summarized in Table I which presents, for various R values, the potential energies V_A and V_B corresponding to states "A" and "B." Other columns in Table I give the correspondingly calculated values $(\theta T)_A$ and $(\theta T)_B$ in the two cases.[21] Here, θT is given in deg keV, laboratory coordinates.

Evidently a given scattering angle can correspond to two different impact parameters, or even to a range of impact parameters.[22] This makes it difficult in principle to apply the impact parameter method theory to the

TABLE I. At various values of internuclear separation R, or distance of closest approach R_0, calculated values for the HeH$^+$ system are given for the potential energies $V(R)$ and the product θT of scattering angle and incident energy. Here, "A" refers to the singlet ground state of HeH$^+$ and "B" refers to the next singlet state. The subscript "av" refers to the average value, and the subscript "R" refers to Rutherford scattering.

R or R_0 (Å)	$V_A(R)$ (eV)	$V_B(R)$ (eV)	$(\theta T)_A$ (deg keV)	$(\theta T)_B$ (deg keV)	$(\theta T)_{av}$ (deg keV)	$(\theta T)_R$ (deg keV)
0.01	2650	2750	165	165	165	165
0.02	1330	1350	83	83	83	83
0.04	608	636	40	40	40	41
0.06	365	410	25.8	26.2	26.0	27.5
0.10	181	226	14.4	15.0	14.7	16.5
0.15	96	140	8.6	9.2	8.9	11.0
0.20	53	95	5.2	6.5	5.9	8.3
0.30	18.5	55	2.0	4.0	3.0	5.5
0.40	6.0	37.5	0.8	2.9	...	4.1
0.50	+1.0	27.5	...	2.2	...	3.3
0.60	−0.4	21.2	...	1.8	...	2.8

[14] A. A. Evett, J. Chem. Phys. **24**, 150 (1956).

[15] R. Bhattacharya, Proc. Natl. Inst. Sci. India **A27**, 185 (1961).

[16] B. G. Anex, J. Chem. Phys. **38**, 1651 (1963).

[17] H. H. Michels and F. E. Harris, J. Chem. Phys. **39**, 1464 (1963). See their Table IV.

[18] H. H. Michels (to be published), and Bull. Am. Phys. Soc. **9**, 232 (1964). The present authors appreciate the opportunity to use the results of Michels' calculations in advance of publication.

[19] D. R. Bates and T. R. Carson, Proc. Roy. Soc. (London) **A234**, 207 (1956).

[20] T. A. Green, Sandia Corporation, Albuquerque (private communication).

[21] A difficulty arises in the calculation of $(\theta T)_A$. The ground state is stable and the interatomic force changes sign at the equilibrium distance. There is, therefore, a value of R_0 somewhat less than the equilibrium distance for which the incident particle receives equal and opposite deflections along its path such that the net deflection is zero. Thus, $(\theta T)_A$ reaches zero and changes sign at a value of R_0, which is in the vicinity of 0.5 Å. The calculation for $R > 0.4$ Å is not carried out here because our data are concerned with smaller values of R_0, where repulsive forces predominate strongly.

[22] Recently Felix T. Smith, Bull. Am. Phys. Soc. **9**, 411 (1964), and Francis J. Smith, Phys. Letters **10**, 290 (1964) have studied the consequences of similar considerations in the symmetric cases of He$^+$ on He and H$^+$ on H, respectively.

present data. However, at the higher θT values, $(\theta T)_A$ and $(\theta T)_B$ do not differ greatly at constant R_0. It seemed reasonable, therefore, to average these to obtain an approximate relationship, $(\theta T)_{av}$ versus R_0, to use in discussing the data. This is equivalent to assuming that the system is in state "A" during the first half of the collision, the transition occurs, and then the system is in state "B" during last half of the collision. These average values are given in Table I. At the larger R_0 values, where this average has little meaning, the $(\theta T)_{av}$ values are omitted.

The last column in this table gives, for comparison, the values $(\theta T)_R$ for Rutherford scattering wherein the above complications involving electronic energies are entirely neglected.

4. DISCUSSION

The theory will be briefly discussed before the two particular reactions (1) and (2) are considered.

(a) Nonresonant Collisions

The general theory is that of Bates, Massey, and Stewart[6] who present formulas for the transition probability between any two states during the collision. In the impact parameter formulation, these probabilities involve an oscillatory term which depends on the energy difference between the two states in question, and another factor which is an integral (over the electron coordinates) of the product of one molecular wave function with the derivative of the other with respect to internuclear separation. An important improvement in the theory was made by Bates and McCarroll,[8] who pointed out the changes which arise from taking into account the initial linear momentum of the active electron in the center-of-mass frame.

Takayanagi's paper[7] is concerned with calculations of total cross section for nonresonant charge transfer wherein expansions are made in atomic orbitals. His results for the H$^+$ on He collisions are in fairly good
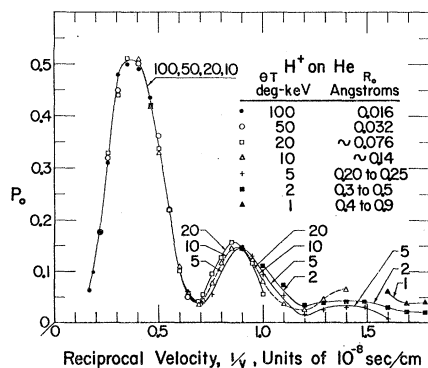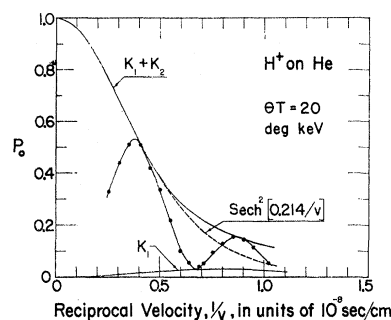
FIG. 5. For H$^+$ on He collisions, the electron capture probability P_0 is plotted versus $1/v$, the reciprocal of the incident proton velocity. These data are for the particular case where the product of scattering angle θ and incident energy T is 20 deg-kV. An upper envelope K_1+K_2 and a lower envelope K_1 are shown. The dashed line is an analytic expression shown for comparison with K_1+K_2.

agreement with experiment. However, his intermediate results for differential cross section are not given, and it would not be expected that atomic orbitals would be suitable to describe collisions at small impact parameters.

Detailed calculations by Bates and Lynn[9] are concerned with electron capture in nonresonant cases where the energy defect happens to be nearly zero, and are not intended to apply in the present case where ΔE is 11 eV. Rapp and Francis[10] discuss symmetry principles in H$^+$ on He collisions, and make an approximate calculation (using atomic wave functions) of the electron capture probability. Their calculation is reasonably accurate at large impact parameters, but is not applicable to the present study of small impact parameter collisions. Demkov[11] presents an approximate calculation using atomic wave functions which applies in cases where ΔE is small. An order-of-magnitude calculation by Lichten[3,12] and estimates by Rapp[23] both predict that the spacing of the resonance peaks of H$^+$ on He should be intermediate between the spacings observed in the H$^+$ on H and the He$^+$ on He case, and this is qualitatively true. However, there is no reasonably accurate calculation applicable to the present case of small impact parameter and large energy defect.

It is interesting that several theories,[9–11] within the range of their applicability find a result in the form

$$P_0 = \text{sech}^2(C/v) \sin^2(D/v), \tag{4}$$

where v is the velocity and C and D are constants which depend on the impact parameter. It will be seen that the present data do not fit this form very well.

(b) H$^+$ on He

The form of Eq. (4) suggests that P_0 should be plotted versus reciprocal velocity. Such a plot in the resonant case[1,4] shows even spacings of the maxima of P_0. This has been done in Fig. 4, which shows P_0 versus $1/v$

FIG. 4. For H$^+$ on He collisions, the electron capture probability P_0 is plotted versus $1/v$, the reciprocal of the proton velocity. Data are presented wherein the product θT of scattering angle and incident energy is held constant. The corresponding values of distance of closest approach R_0 are indicated.

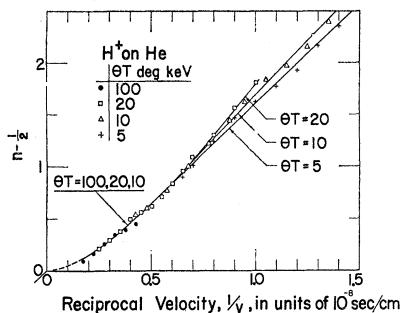[23] D. Rapp (private communication). See also Ref. 10.

FIG. 6. These data are for H^+ on He collisions. A parameter $n-\frac{1}{2}$, (which is a measure of the "number of oscillations during the collision") is plotted versus reciprocal proton velocity $1/v$ (which is a measure of the collision duration). Each value of the parameter θT corresponds, roughly, to a particular impact parameter.

for several values of the parameter θT, corresponding roughly to holding R_0 constant along each of the curves.

A rather flexible empirical equation,

$$P_0 = K_1(1/v) + K_2(1/v)\,\sin^2(n-\tfrac{1}{2})\pi \qquad (5)$$

fits the data. Here K_1 is a slowly varying function of reciprocal velocity which is a lower envelope, and K_1+K_2 is the upper envelope of the data curves. These are shown in Fig. 5 which illustrates the particular case of $\theta T = 20$ deg-keV. In Eq. (5), n is regarded as an empirical continuous function of $1/v$, the points of tangency with the upper envelope occurring for $n=1, 2, 3, \cdots$ and the tangency with the lower envelope occurring at $n=\frac{3}{2},\frac{5}{2},\cdots$. For the case $\theta T = 20$, the values of P_0, K_1, and K_2 may be read from Fig. 5 and used in Eq. (5) to compute $n-\frac{1}{2}$. These values of $n-\frac{1}{2}$ are plotted versus $1/v$ in Fig. 6, which shows the results for other θT values as well.

This procedure is somewhat arbitrary, since $n-\frac{1}{2}$ depends on the particular envelopes K_1 and K_1+K_2 chosen as in Fig. 5. However, the points of tangency with the upper and lower envelopes are fairly accurately located, irrespective of the envelopes. The values of $n-\frac{1}{2}$ are changed only slightly when the envelopes are arbitrarily adjusted within reasonable limits. Detailed study shows that it is impossible to straighten the curves in Fig. 6 without assigning quite grotesque shapes to the envelopes. The curvature in this figure comes about because the first peak in Fig. 4 is "wider" than the second peak.

The curves of Fig. 6 may be thought of as plotting the "number of oscillations" as a function of the "duration of the collision," such curves having been useful in previous studies of the resonant case.[4] The slope of these curves is proportional to the "rate of charge transfer during the collision" and should be of theoretical interest.

It is customary[1,3,4] to multiply the slopes by Planck's constant h, so that they are dimensionally an energy times a length. Table II gives these slopes I in eV Å

TABLE II. Results are given for H^* on He collisions for data wherein the product θT of scattering angle and energy is held constant. For selected values of reciprocal velocity, $1/v$, are given the values of a quantity I, which is the slope of the curves in Fig. 6 times Planck's constant. For reference, rough values of distance of closest approach R_0 are included.

θT (deg keV)	$1/v$ (sec/cm)	I (eV Å)	R_0 (Å)
100	0.2×10^{-8}	49	0.016
100	0.4×10^{-8}	71	0.016
20	0.3×10^{-8}	64	0.077
20	1.0×10^{-8}	101	0.077
10	0.5×10^{-8}	79	0.14
10	1.0×10^{-8}	87	0.14
5	1.0×10^{-8}	80	0.23

units for various θT and $1/v$ values. The decrease in slope at small $1/v$ (fast collisions) is consistent with a phase effect found experimentally by Lockwood and Everhart[1] in the H^+ and H case. This may be explained, following Bates and McCarroll,[2] as arising in the theory when account is taken of the initial momentum of the active electron in the center-of-mass frame.

The $\theta T = 5$ curve lies below the $\theta T = 10$ curve in Fig. 6 with a somewhat lower slope. When θT decreases, R_0 becomes larger so that the interaction is slightly weaker.

The empirical envelope K_1+K_2 does not fit the functional form $\mathrm{sech}^2(C/v)$ very well, although this function, suggested by Eq. (4), does have roughly the right shape and fits the first peak with $C=0.214$ cm/sec as shown by the dashed line in Fig. 5.

In the H^+ on He collision, the molecular states which are presumably of interest are the singlet states marked "A" and "B" on Fig. 3. However, transitions to higher states (including Π states not shown in Fig. 3) may also occur.[24]

(c) He⁺ on H

Reaction (2) is concerned with both singlet and triplet states. Thus, in 25% of the collisions, the initial state is the singlet state "B" in Fig. 3, and transitions can occur to either the ground state "A" or to another singlet state such as "D." If only the singlet reaction occurred P_0 could not possibly be over 0.25. However, Fig. 2 shows much higher values of P_0, and therefore triplet reactions do contribute to the data. In 75% of the collisions the initial state is the triplet state "C" and the transitions which occur can only be to one of the higher triplet states such as "E," which leaves the helium atom excited after the collision.

One would expect that the singlet reaction would cause a peak in this P_0 data at 28 keV, which is at the same relative velocity as the 7-keV peak in the forward reaction H^+ on He. The data of Fig. 2 are inconclusive in this respect. On the same basis, one would also pre-

[24] D. R. Bates and D. A. Williams, Proc. Phys. Soc. **83**, 425 (1964), have shown that Π states make important corrections to the theory in the case of the H^+ and H collision.

dict that the singlet reaction would contribute to a peak at 144 keV in the He^+ on H collision, whose velocity corresponds to the 36-keV peak seen in H^+ on He data.

5. TOTAL CROSS SECTIONS

It is interesting to relate the present differential measurements of the H^+ on He collision with measurements of the total cross section for charge transfer σ_{10} in the same collision.

Stedeford and Hasted[25] and Stier and Barnett[26] give values of σ_{10} which show a single broad peak. The maximum is 1.8×10^{-16} cm^2 and occurs at 23 keV, somewhat below the position of the 36-keV maxima in the differential P_0 data of Fig. 1. These quantities are related by

$$\sigma_{10} = 2\pi \int_0^\pi P_0(\theta)\sigma(\theta)\sin\theta d\theta \qquad (6)$$

or, alternatively, by

$$\sigma_{10} = 2\pi \int_0^\infty P_0(\rho)\rho d\rho, \qquad (7)$$

where $\sigma(\theta)$ is the differential cross section for scattering of all particles, irrespective of their charge state, and ρ is the impact parameter.

The maxima of σ_{10} and P_0 do not coincide, and the oscillatory nature of the P_0 data is not reflected in the σ_{10} data. This situation can occur because the major portion of the contribution to total cross section arises from scattering at angles smaller than those measured in the present study. A numerical example will illustrate this: At 23 keV, P_0 is about 0.38 for all angles greater than $\frac{1}{2}°$. Taking $\theta T = (\frac{1}{2})$ (23) in Table I, one finds R_0 to be 0.13 Å, which is substantially equal to the corresponding impact parameter ρ_1. The contribution for $\rho \leq \rho_1$ in Eq. (7) is $P_0\pi\rho_1^2$, which is about 0.02×10^{-16} cm^2, using the numbers above. The total cross section quoted at this energy is almost 100 times larger. Thus only about 1% of the total cross section arises from scattering at angles of $\frac{1}{2}°$ or greater in this case.

It is difficult to obtain differential data at angles much smaller than $\frac{1}{2}°$, and detailed experimental study of the integrand of Eq. (6) at angles near zero, though not impossible in principle, will require new techniques.

The application of the other expression, Eq. (7), is beset by two additional considerations which make it extremely difficult, perhaps impossible in principle, to make an experimental verification at large impact parameters of formulas developed by impact parameter-method theories:

(1) The lack of one-to-one correspondence between θT and ρ (or R_0), discussed above in Sec. 3, causes serious problems in relating data and theory.

(2) At very small scattering angles, diffraction effects arise, and application of the uncertainty principle shows that the impact parameter cannot be inferred from angular scattering measurements.[27] Although Eq. (7) is often used to calculate total cross sections, it is impossible experimentally to measure the integrand in Eq. (7) in the region which contributes most heavily to the total cross section.

Entirely apart from their relationship to total cross sections, these close encounters are interesting *per se*. The impact parameter theories are properly applicable to the present experiments especially in predicting the P_0 results for impact parameters near zero.

ACKNOWLEDGMENTS

[25] J. B. H. Stedeford and J. B. Hasted, Proc. Roy. Soc. (London) A227, 466 (1955).
[26] P. M. Stier and C. F. Barnett, Phys. Rev. 103, 896 (1956).

[27] This difficulty as applied to He^+ on He scattering is discussed in more detail in a paper by E. Everhart, H. F. Helbig, and G. J. Lockwood, in *Proceedings of the Third International Conference of the Physics of Electronic and Atomic Collisions*, edited by M. R. C. McDowell (North-Holland Publishing Company, Amsterdam, 1964), p. 865.